

Design of Sliding Mode Controllers using Reduced-order Koopman Mode Representations

Sachit Rao* Debasish Ghose**

* *International Institute of Information Technology - Bangalore, Bangalore, India 560 100 (e-mail: sachit@iiitb.ac.in).*

** *Department of Aerospace Engineering, Indian Institute of Science, Bangalore, India 560 012 (e-mail: dghose@iisc.ac.in)*

Abstract: The Koopman operator framework allows for a linear, but infinite-dimensional, representation of the dynamics of a non-linear system. The Koopman modes, or observables, and the resulting linear dynamics are derived purely using a data-driven framework, where the data are system outputs measured at discrete samples; improving accuracy of the Koopman representation requires a large number of such modes to be considered. Recent results consider the system input as well, in the derivation of the discrete linear dynamics, thus enabling the design of controllers. Sliding mode controllers (SMCs), including the discrete-time versions, can handle parameter uncertainties and variations and also ensure that the control objective is satisfied in finite time. In this paper, a discrete-time SMC is designed for the output control of a dynamic system approximated by fewer Koopman modes; the SMC is expected to handle uncertainties introduced by the ignored modes. Conditions are identified for the closed-loop system to be stable, with the occurrence of sliding mode.

Copyright © 2023 The Authors. This is an open access article under the CC BY-NC-ND license (<https://creativecommons.org/licenses/by-nc-nd/4.0/>)

Keywords: Sliding mode control; Data-driven control; Nonlinear system identification; Identification for control; Model reduction.

1. INTRODUCTION

As is well known from the literature, Koopman operator theory permits a non-linear dynamic system to be represented by a linear dynamic system, albeit with infinite dimensions. As mentioned in Proctor et al. (2018), with the inclusion of inputs acting on the non-linear system within the Koopman framework, this approach provides linear dynamics, whose properties are estimated purely from input-output data. By constructing the *observables* - which are non-linear functions of the states of the original non-linear system - from such data, that lead to the linear system representation, controllers applicable to linear systems can be designed to control the non-linear system. Indeed, the Koopman approach has found many applications, for example, control and observer design using a bilinear approximation, in Goswami and Paley (2022) and Surana (2016), respectively; modeling the working environment for autonomous excavators in Sotiropoulos and Asada (2022); and in robotics and motion control of rigid bodies, Mamakoukas et al. (2019); Bruder et al. (2019); Zinage and Bakolas (2022).

The challenges with the application of the Koopman theory are the choices of observables and how many should be selected to result in a better approximation. A solution to overcome these challenges is proposed by Korda and Mezić (2018), where, by *lifting* the state-space of the non-linear system to a higher-dimensional one, the dynamics in the lifted space of observables become linear; the observables are selected in the form of radial basis

functions. The resulting linear system is now considered as a predictor and using least-squares-based methods, the parameters of the predictor are estimated so that its trajectories closely match the trajectories of the non-linear system. See also Korda and Mezić (2020); Williams et al. (2016); Kaiser et al. (2021) for other approaches and their descriptions, such as the Dynamic Mode Decomposition (DMD), the Extended DMD, and KRONIC, that enable Koopman-type representations.

From the above remarks, it is clear that diverse approaches result in different linear system representations of the same non-linear system. However, from a feedback control perspective, if the objective of control is for the output of the linear system to track a reference signal - either time-varying or a fixed point - then the control should be designed to meet this objective by considering the internal dynamics as well as the composition of the output itself as being uncertain. From this point-of-view, SMCs seem an appropriate design choice. In particular, discrete-time SMCs should be applied, since the input-output data - used to construct the Koopman representation - are available at discrete samples, thus leading to a discrete-time linear representation. For linear systems, the notion of the so-called Discrete Sliding Mode (DSM), is well understood; see Drakunov and Utkin (1989); Furuta (1990) for DSM controller designs; the sliding manifold is selected so that the closed-loop system has the desired dynamics. The benefits offered by the enforcement of DSM is that it occurs after a finite number of time instants and that it is robust to plant uncertainties; see Bartolini

et al. (1995) for design of adaptive DSM controllers that handle plant uncertainties explicitly. In the literature, only the Linear Quadratic Regulator (LQR) or the Model Predictive Controller (MPC), have been designed and implemented for Koopman approximations.

From a DSM controller design viewpoint itself, the linear Koopman representation simplifies the design process in two ways. First, the need to solve non-linear equations is eliminated. Formally, for discrete-time non-linear systems, the so-called *equivalent control* - which forms a key component of the overall DSM controller - is computed by solving a set of non-linear equations (the dynamic equations), Rubagotti et al. (2021); also see Zheng et al. (2007), where a non-linear system is first expressed as a sum of local linear models - using the Takagi-Sugeno fuzzy approach - and a DSM controller is now designed for the linear model. The step of solving non-linear equations to calculate control is eliminated for linear systems, as now, the equivalent control can be computed using matrix products and inverses. Second, the Koopman observables are available for control computation and not just the system outputs; with the former, there is now no need for observers to estimate internal states. With both these features of the Koopman representation, pole-placement methods, that allow for arbitrary selection of the closed-loop poles, or even LQR-type methods can be used to design the sliding manifold.

The contributions of the paper are as follows:

- (1) The use of the linear Koopman representation to design DSM controllers for non-linear systems, which is in contrast to nearly all other results in the literature which present designs of MPC or LQR-type controllers.
- (2) The use of DSM controller design techniques to control the outputs - by enforcing them to lie on a manifold - of “approximate” linear Koopman representations themselves. This aspect is crucial as different approximation techniques result in different representations - hence, the dynamics may be considered to be uncertain.
- (3) Study on the use of a reduced-order Koopman model in the design of the DSM controller and sliding manifold. The occurrence of sliding mode restricts the behaviour of the output according to the chosen manifold so that the dynamics of the ignored modes, even in the closed-loop, do not influence the output.

In addition, the DSM controller considers bounds on the control input. This is required as the magnitude of control tends to infinity as the sampling time reduces, Drakunov and Utkin (1989). As MPCs inherently include such bounds in their computation, this is the most prevalent control approach presented in the literature for the control of Koopman systems.

In this paper, a DSM controller design is demonstrated for the control of the Koopman representation of the discrete Damped Duffing Oscillator. The linear system matrices are derived using the approach - and the code - described in Korda and Mezić (2018). Various orders of observables are considered, for which both a full-order and a reduced-order DSM controller are designed.

The paper is organised as follows: in Sec. 2, the Koopman operator theory is briefly described for both uncontrolled and controlled systems. The design of the DSM controller is presented in Sec. 3 and the aspects of computation of the equivalent control for linear and non-linear systems are distinguished. Simulation results are presented in Sec. 4, followed by Conclusions in Sec. 5.

2. KOOPMAN OPERATOR THEORY

As the Koopman representations used in this paper are derived from Korda and Mezić (2018), the notations used here are also similar, but some additional notations from Kaiser et al. (2021) are also used. Consider an discrete-time, non-linear, uncontrolled system of the form $x^+ = f(x)$, $x \in \mathfrak{R}^n$, where the function f is the mapping of the transitions of the state x ; also denoted as the flow map. Given a set of measurement functions $\phi : \mathfrak{R}^n \rightarrow \mathfrak{R}$ of the states x in the space \mathcal{F} , the linear and infinite-dimensional Koopman operator $\mathbf{K} : \mathcal{F} \rightarrow \mathcal{F}$ satisfies $\mathbf{K}\phi = \phi(f(x))$, that is, the measurement functions can be updated in discrete-time according to $\phi^+ = \mathbf{K}\phi$. The measurement functions ϕ are also denoted as the *observables*. The Koopman operator retains all properties of the dynamics of the non-linear system, if the functions ϕ contain information on the states x . Thus, for the right choice of observables found from measured data - and the number of such observables may be infinite - the non-linear system can be expressed as a linear dynamical system.

As the Koopman operator is linear, its eigenfunctions and corresponding eigenvalues, denoted by $\mathbf{K}\psi_i = \lambda_i\psi_i$, can be found. The Koopman eigenfunctions satisfy the property $\lambda_i\psi_i = \psi_i(f(x))$. Thus, if the observables, ϕ , match the eigenfunctions, ψ , then, the non-linear dynamics can be represented by a linear one that holds globally. For example, the system $x_1^+ = \mu x_1$, $x_2^+ = \nu(x_2 - x_1^2)$ can be represented by a finite-dimensional linear Koopman form using the eigenfunctions (or observables) $\psi_1 = x_1$ and $\psi_2 = (x_2 - \kappa x_1^2)$, $\kappa = \nu/(\nu - 2\mu)$; this choice yields the linear dynamics $\psi_1^+ = \mu\psi_1$, $\psi_2^+ = \nu\psi_2$. Note that as μ, ν are estimated from input-output data, they can be uncertain. As has been recognised in the literature, finding these eigenfunctions, in essence, the “right” observable functions is a key challenge. These are typically approximated as a combination of candidate functions, say in the form of polynomials, or radial basis functions.

For systems with control, of the form $x^+ = f(x, u)$, $u \in \mathfrak{R}^m$, in identifying the Koopman representation, the value of control u at every instant is appended to the vector of observables $\phi(x)$ to form a new vector, χ . This procedure is applicable for systems that do not depend on the derivatives of control, although systems with control dynamics can also be converted into the Koopman form, see Proctor et al. (2018) for details. Following the procedure described in Korda and Mezić (2018), the observable functions for the states χ are chosen to be linear with respect to control. Since the interest is in deriving the time-domain representations of the non-linear system, predictors of the form

$$z^+ = \mathbf{A}z + \mathbf{B}u \quad (1a)$$

$$y = \mathbf{C}z, \quad y \in \mathfrak{R}^p, \quad (1b)$$

are determined from data $x(0), x(1), \dots$ and $u(0), u(1), \dots$. Applying least-squares methods yields the matrices \mathbf{A} , \mathbf{B} , and \mathbf{C} . The vector $z = [\psi_1(x) \dots \psi_N(x)]^T \in \mathbb{R}^N$, where $N \gg n$ (typically) is the number of observable functions that yields the Koopman approximation.

In this paper, the discrete-time predictor (1) is used to design the control u as a DSMC to meet the control objective, say $z \rightarrow 0$. It is highlighted that the entire vector z is available to compute the control policy, thus output feedback-based DSM controllers, such as designed in Edwards and Spurgeon (2002), are also not needed; note that such output-based controllers require the system parameters to satisfy special conditions to design controllers. As will be presented in Sec. 4, different types and orders (N) of the observables lead to different system matrices, thus rendering the original non-linear system as being uncertain. For such systems, sliding mode control is an appropriate choice.

3. DISCRETE SLIDING MODE CONTROL

From Drakunov and Utkin (1989); Bartolini et al. (1995), for the discrete-time linear system $x^+ = \mathbf{F}x$, $x \in \mathbb{R}^n$, DSM occurs on the manifold $s(x) = 0$, $s \in \mathbb{R}^m$, if there exists an open-neighbourhood $U \in \mathbb{R}^n$, such that $s(\mathbf{F}x) = 0 \forall x \in U$. For the linear system with control $x^+ = \mathbf{A}x + \mathbf{B}u$, $u \in \mathbb{R}^m$, by defining the sliding manifold as $s(k) = \mathbf{C}_s x(k)$, DSM is enforced by selecting the control as the solution to $s(k+1) = 0$. Since the control magnitudes are usually bounded, in the form $\|u(k)\| \leq u_{\text{lim}}$, the DSM controller is implemented according to the piecewise-constant form

$$u(k) = \begin{cases} u_{eq}(k) & \text{if } \|u_{eq}(k)\| \leq u_{\text{lim}} \\ -u_{\text{lim}} \frac{u_{eq}(k)}{\|u_{eq}(k)\|} & \text{otherwise} \end{cases} \quad (2)$$

where $u_{eq}(k) = -(\mathbf{C}_s \mathbf{B})^{-1} \mathbf{C}_s \mathbf{A}x(k)$; $u_{eq}(k)$ can be interpreted as equivalent control, that is well-defined for continuous-time systems. The sliding manifold parameters \mathbf{C}_s are selected so that the matrix $(\mathbf{I} - \mathbf{B}(\mathbf{C}_s \mathbf{B})^{-1} \mathbf{C}_s) \mathbf{A}$, that defines the closed-loop dynamics, has the desired properties.

The DSM controller (2) can also suppress bounded disturbances acting on the system, so that the DSM becomes invariant to them, if matching conditions are satisfied.

While various design strategies are available to design $u(k)$, since the focus of this paper is in the implementation of DSM controllers to Koopman representations, the control policy according to (2) is used in this paper. Most, however, still require calculation of the equivalent control u_{eq} as the solution to $s(k+1) = 0$. As discussed in Rubagotti et al. (2021), for a control system of the form $x^+ = f(x, u)$, with sliding manifold $s = S(x) = 0$, equations of the form $S(f(x, u_{eq})) = 0$ need to be solved to obtain u_{eq} . For control-affine systems and sliding manifolds that are linear functions of the state x , u_{eq} can be calculated analytically.

3.1 Design in the Regular Form

The sliding manifold matrix $\mathbf{C}_s \in \mathbb{R}^{m \times n}$ can be selected in the form $[\mathbf{K} \ \mathbf{I}_m]$, where, $\mathbf{K} \in \mathbb{R}^{(n-m) \times m}$, by transforming the original linear system to the so-called regular form

$$x_1^+ = \mathbf{A}_{11}x_1 + \mathbf{A}_{12}x_2 \quad (3a)$$

$$x_2^+ = \mathbf{A}_{21}x_1 + \mathbf{A}_{22}x_2 + \mathbf{B}_2u, \quad (3b)$$

using an appropriate transformation matrix; see Appendix A for the derivation of this matrix. In (3), $x_1 \in \mathbb{R}^{(n-m)}$, $x_2 \in \mathbb{R}^m$. Now, if the pair $(\mathbf{A}_{11}, \mathbf{A}_{12})$ is controllable and the matrix $\mathbf{B}_2 \in \mathbb{R}^{m \times m}$ is invertible, then, by enforcing sliding mode on $s(k) = [\mathbf{K} \ \mathbf{I}_m] [x_1(k) \ x_2(k)]^T = 0$, by choosing $u(k)$ according to (2), the sliding mode dynamics, of order $(n-m)$, are given by $x_1^+ = (\mathbf{A}_{11} - \mathbf{A}_{12}\mathbf{K})x_1$. The matrix \mathbf{K} can now be selected based on the pole-placement method, so that the closed-loop dynamics has the desired transient behaviour. Note that as the pair $(\mathbf{A}_{11}, \mathbf{A}_{12})$ is assumed to be controllable, arbitrary pole-placement can be performed.

3.2 Design for Koopman Systems

The procedure described in Sec. 2 yields the approximate linear predictor, (1), for the non-linear system $x^+ = f(x, u)$. Now, by transforming (1) to the regular form (3), say with states z_1 and z_2 , with appropriate dimensions, a discrete sliding manifold and corresponding controller can be designed so that control objectives, say $z_{1,2} \rightarrow 0$, can be met.

The motivation to design DSM controllers for Koopman systems stems from the robustness properties that can be assigned to the sliding manifold dynamics. Now, as mentioned before, the linear predictor (1) is an approximation of the true non-linear system. Suppose it is possible to express the predictor matrices in the form $\mathbf{A} = \mathbf{A}_{true} + \Delta\mathbf{A}$, and $\mathbf{B} = \mathbf{B}_{true} + \Delta\mathbf{B}$, where \mathbf{A}_{true} and \mathbf{B}_{true} capture the dominant spectral properties of the non-linear dynamics and the matrices $\Delta\mathbf{A}$ and $\Delta\mathbf{B}$ are uncertain, then design techniques, such as presented in Zheng et al. (2007), can be adopted to design the DSM controller.

Without any loss of generality, let the control objective be to make $x \rightarrow 0$, where, $x \in \mathbb{R}^n$ are the states of the non-linear system. Now, the observables ψ chosen to approximate this system are expected to contain information on the states of the non-linear system. If n (which denotes the number of states of the non-linear system) of the observables, ψ_i , $i = 1, \dots, N_O$, where $N_O \gg n$, satisfy $\psi_i = x_i$ (that is, these n observables are the states themselves and not functions of the states), then ensuring that all the observables $\psi_i \rightarrow 0$, by applying the DSM controller, implies that the primary control objective of making $x \rightarrow 0$ is satisfied. Indeed, it is necessary for the linear predictor to satisfy the fundamental property of full state controllability.

From a generic feedback control perspective, the Koopman operator theory is able to capture the spectral properties of the original non-linear system - these are given by the eigenvalues of the corresponding Koopman eigenfunctions. Thus, if some of these eigenvalues lie outside the unit circle then these eigenfunctions (or observables) can be explicitly considered in the linear representation and the stable eigenfunctions, say those that decay rapidly, can be ignored.

The results of designing a DSM controller for various Koopman representations of the Duffing equation are presented next.

4. SIMULATION RESULTS

In this section, we design DSM controllers for the Damped Duffing Oscillator (DDO), defined by the discrete non-linear dynamics,

$$x_1^+ = x_1 + \Delta t x_2 \stackrel{\text{def}}{=} f_1 \quad (4a)$$

$$x_2^+ = \Delta t x_1 - 4\Delta t x_1^3 + (1 - 0.5\Delta t)x_2 + 0.5\Delta t u, \quad (4b)$$

$$\stackrel{\text{def}}{=} f_2 + gu,$$

where $x_1, x_2 \in \mathfrak{R}$ are the states, $u \in \mathfrak{R}$ is the control, and $\Delta t = 0.01$ sec is the step-size used to discretise the continuous non-linear dynamics. The control objective is to stabilise the states at $(0, 0)$, which is an unstable equilibrium.

4.1 Control of the Non-linear System

A DSM controller is designed for the non-linear dynamics (4). The sliding manifold is selected as $s(k) = cx_1(k) + x_2(k)$, where $c > 0$ decides the transient properties of the sliding mode dynamics. The control is implemented according to the piecewise-constant form (2), where, the equivalent control is given by

$$u_{eq}(k) = -g^{-1}(f_2 + cf_1), \quad (5)$$

and $g, f_{1,2}$ are defined in (4). The results of implementing this DSM are shown in Fig. 1 with $c = 0.95$ and $u_{lim} = 2$; different values of c yield different transient characteristics. It can be observed that the DSM occurs after a finite number of steps and that the control bounds are maintained.

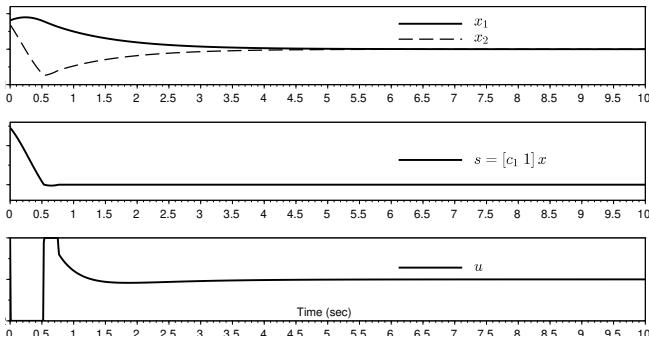


Fig. 1. Control of the non-linear system using a DSM controller

4.2 Control of the Koopman Predictors

Following the procedure described in Korda and Mezić (2018) and the programs available in Korda (2020), the system matrices of the predictor (1) are calculated. For the results presented in this paper, the number of observables are varied; as the code presented in Korda (2020) uses radial basis functions (also of several types), the **gauss** type of function is selected to define the states of the predictor. While this choice of basis function is made arbitrarily, the impact of designing a DSM controller for this uncertain system becomes evident.

The orders of the observables, $z \in \mathfrak{R}^{N_O}$, are selected as $N_O = 8$ and $N_O = 16$. The open-loop evolution of the states $x_{1,2}$, given by the non-linear dynamics (4) and the outputs of the Koopman predictor, are shown in Fig. 2. As can be seen, the predictor with $N_O = 16$ approximates the non-linear system better than $N_O = 8$; this result is similar to the ones presented in Korda and Mezić (2018, 2020).

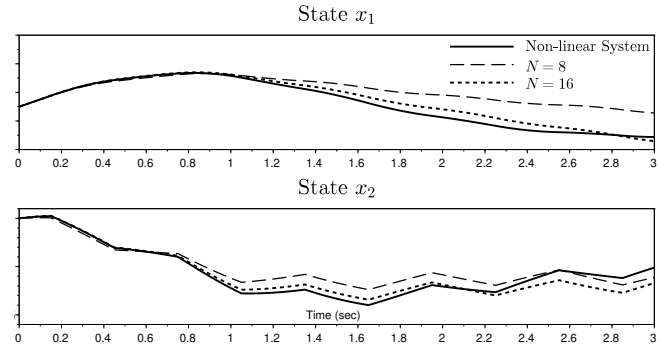


Fig. 2. Open-loop outputs of the DDO using the non-linear model and Koopman representations with different orders (N) of the predictor; a square wave input is applied

The DSM controller is designed using the Regular Form technique presented in Sec. 3. Prior to performing pole-placement to evaluate the matrix \mathbf{K} , the controllability of the full-order predictor and the reduced-order system in the regular form is examined. The variation in the rank of the respective controllability matrices with number of observables, N , selected to define the linear system, is shown in Fig. 3. To generate these results, the predictor with order $N_O = 16$ and different sub-matrices of different orders are selected from the pair, (\mathbf{A}, \mathbf{B}) , found with $N_O = 16$. These sub-matrices are obtained by partitioning the $N_O \times N_O$ matrix \mathbf{A} and the $N_O \times 1$ matrix \mathbf{B} in the form

$$\mathbf{A} = \begin{bmatrix} \mathbf{A}_1 & \mathbf{A}_2 \\ \mathbf{A}_3 & \mathbf{A}_4 \end{bmatrix}, \quad \mathbf{B} = \begin{bmatrix} \mathbf{B}_1 \\ \mathbf{B}_2 \end{bmatrix} \quad (6)$$

where $\mathbf{A}_1 \in \mathfrak{R}^{N \times N}$ and $\mathbf{B}_1 \in \mathfrak{R}^{N \times 1}$ with $n \leq N \leq N_O$; the other matrices in (6) are of appropriate dimensions.

As can be seen in Fig. 3, the system loses full controllability for some values of N ; note that the rank of the controllability matrix of the pair $(\mathbf{A}_{11}, \mathbf{A}_{12})$ (derived from expressing the system with matrices $(\mathbf{A}_1, \mathbf{B}_1)$ in the regular form) is *one less* (dimension of control) than that of the full-order predictor.

Note that controller design can still be performed for the system that is not fully controllable by partitioning the states into the controllable and uncontrollable states using standard Kalman decomposition techniques. Indeed, the uncontrollable states should be stable in such cases, although this case is not considered in this paper.

A DSM controller is designed for $N = 8$ states of the predictor estimated using $N_O = 16$ observables. The results of implementation are shown in Fig. 4. The matrix \mathbf{K} , in the definition of the sliding manifold, is chosen such that the reduced-order closed-loop matrix $(\mathbf{A}_{11} - \mathbf{A}_{12}\mathbf{K}) \in \mathfrak{R}^7$ has the desired eigenvalues; these eigenvalues are randomly chosen from the range $[0.6 \ 0.95]$.

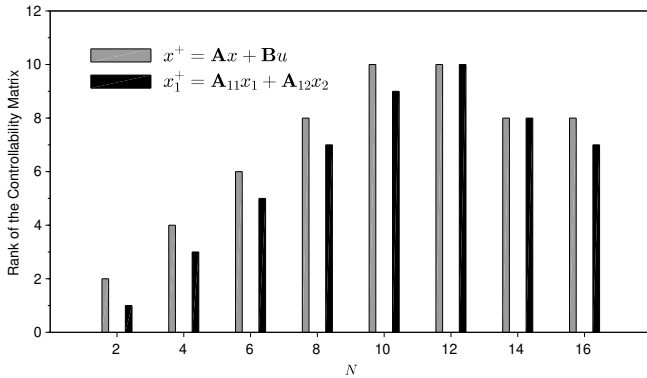


Fig. 3. Variation in the rank of the controllability matrices with number of states in the predictor

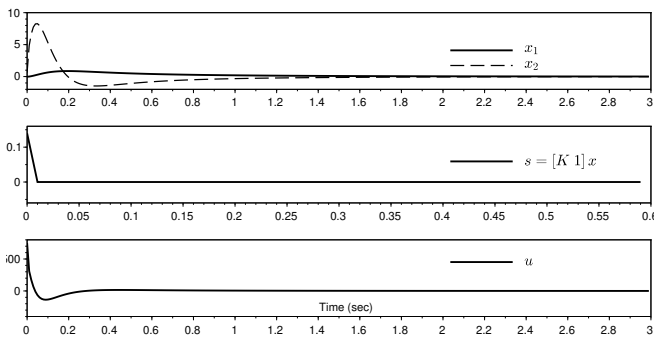


Fig. 4. Closed-loop control using a DSM controller for a predictor with $N = 16$ states, but choosing only the first 8 states

To enforce sliding mode on $s(k) = 0$, the bound on control had to be increased considerably. This can be observed from the magnitude of control determined in the reaching phase, in Fig. 4. Reducing this bound led to unstable closed-loop characteristics. While this result deserves closer analysis, and is out of scope of this paper, potential reasons could be the magnitude of the coefficient multiplying the control input that appears in the regular form design as well as the sampling interval used to calculate the DSM controller (0.01 sec in this case). However, the DSM controller is able to steer the outputs of the DDO system to the desired values.

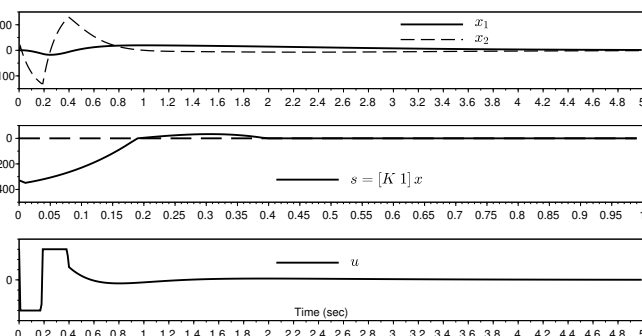


Fig. 5. Closed-loop control using a DSM controller for a predictor with $N = 8$ states, but choosing only the first 6 states

Similar results can be observed when the number of states in the observer is selected as $N_O = 8$. Even for this case, the system lost full state controllability, and hence the first 6 ($N = 6$) states are selected. These results are shown in Fig. 5. In this case, a larger control magnitude was also required.

Finally, a DSM controller is designed for the case where only those modes that correspond to unstable eigenvalues of the open-loop system - defined by matrix \mathbf{A} of the predictor - are considered in the controller design. This result is illustrated for $N = 4$ observables, derived using the predictor with $N_O = 16$ observables; see (6) for the resulting system matrices. This system, with pair $(\mathbf{A}_1, \mathbf{B}_1)$ has 3 unstable eigenvalues; hence, it is first converted to the diagonal form, $x_d^+ = \Lambda x_d + \mathbf{B}_d u$, using the transformation $x_d = \mathbf{V}^{-1}x$, where \mathbf{V} is the matrix of eigenvectors of \mathbf{A}_1 and Λ are its eigenvalues. Thus, this system is of the form

$$x_{di} = \lambda_i x_{di} + b_i u, \quad x_{di} \in x_d, \quad i = 1, \dots, 4. \quad (7)$$

Let, $\lambda_{1,2,3}$ be the unstable eigenvalues. The DSM controller is designed for the 3 states, $x_{d1,2,3}$, again using pole-placement following the Regular Form approach. As a result, with the occurrence of sliding mode on the designed manifold, the states $x_{di} \rightarrow 0$, $i = 1, 2, 3$, as well as the control $u \rightarrow 0$. Now, since the dynamics of the state x_{d4} is asymptotically stable and its input, u , also tends to zero, the state $x_{d4} \rightarrow 0$ at a rate decided by λ_4 . The results of this controller implementation are shown in Fig. 6.

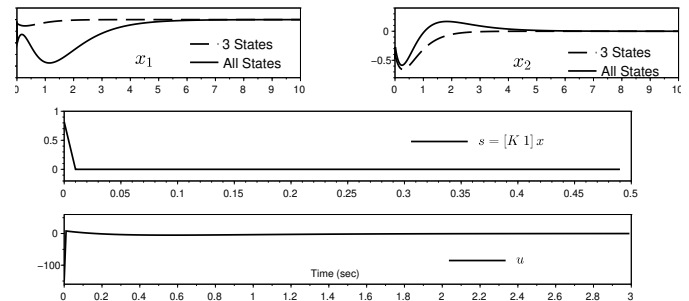


Fig. 6. Closed-loop control using a DSM controller for a predictor where only the unstable modes are controlled; the stable mode is part of the system, but is not considered in controller design

In Fig. 6, the evolution of the states $x_{1,2}$ of the non-linear system are shown when the ignored mode is part of the output and also when it is not, that is, $x_i = C_i x_{d1,2,3}$ and $x_i = C_i x_{d1,2,3,4}$, where C_i is the corresponding output matrix defined in the predictor equations. As can be seen, although the outputs display stable behaviour, when the stable mode is ignored, the transient behaviour is markedly different than when it is not.

5. CONCLUSION

This paper presented the application of the concept of sliding modes to the control of Koopman representations of non-linear dynamical systems with inputs. While the resulting linear dynamics simplifies controller design - as pole-placement can be performed and no observers are needed - the use of Koopman forms illuminates further

avenues of research in the design of DSM controllers. For instance, how does the choice of observables influence transient behaviour as well as the bounds on control that can ensure the occurrence of sliding mode. While alternative DSM controller designs can be implemented that can possibly overcome these challenges, such basic questions still remain. The results presented in this paper will hopefully motivate improved designs of SM controllers for linear systems as well as for output feedback control-based designs.

REFERENCES

- Bartolini, G., Ferrara, A., and Utkin, V. (1995). Adaptive sliding mode control in discrete-time systems. *Automatica*, 31(5), 769–773. doi:10.1016/0005-1098(94)00154-B.
- Bruder, D., Gillespie, B., Remy, C.D., and Vasudevan, R. (2019). Modeling and Control of Soft Robots Using the Koopman Operator and Model Predictive Control. In *Proceedings of Robotics: Science and Systems*. Freiburg im Breisgau, Germany. doi:10.15607/RSS.2019.XV.060.
- Drakunov, S. and Utkin, V. (1989). On Discrete-Time Sliding Modes. *IFAC Proceedings Volumes*, 22(3), 273–278. doi:10.1016/S1474-6670(17)53647-2. Nonlinear Control Systems Design, Capri, Italy, 14–16 June 1989.
- Edwards, C. and Spurgeon, S. (1998). *Sliding Mode Control: Theory And Applications (1st ed.)*. CRC Press. doi:10.1201/9781498701822.
- Edwards, C. and Spurgeon, S. (2002). *Sliding Mode Control in Engineering*, chapter Dynamic Sliding Mode Control and Output Feedback. Marcel Dekker, Inc., New York, Basel. doi:10.5555/560175.
- Furuta, K. (1990). Sliding mode control of a discrete system. *Systems & Control Letters*, 14(2), 145–152. doi:10.1016/0167-6911(90)90030-X.
- Goswami, D. and Paley, D.A. (2022). Bilinearization, Reachability, and Optimal Control of Control-Affine Nonlinear Systems: A Koopman Spectral Approach. *IEEE Transactions on Automatic Control*, 67(6), 2715–2728. doi:10.1109/TAC.2021.3088802.
- Kaiser, E., Kutz, J.N., and Brunton, S.L. (2021). Data-driven discovery of Koopman eigenfunctions for control. *Machine Learning: Science and Technology*, 2(3). doi:10.1088/2632-2153/abf0f5.
- Korda, M. (2020). Koopman MPC. <https://github.com/MilanKorda/KoopmanMPC/raw/master/KoopmanMPC.zip>. Accessed: 8th Nov 2022.
- Korda, M. and Mezić, I. (2018). Linear predictors for nonlinear dynamical systems: Koopman operator meets model predictive control. *Automatica*, 93, 149–160. doi:10.1016/j.automatica.2018.03.046.
- Korda, M. and Mezić, I. (2020). Optimal Construction of Koopman Eigenfunctions for Prediction and Control. *IEEE Transactions on Automatic Control*, 65(12), 5114–5129. doi:10.1109/TAC.2020.2978039.
- Mamakoukas, G., Castano, M., Tan, X., and Murphey, T. (2019). Local Koopman Operators for Data-Driven Control of Robotic Systems. In *Proceedings of Robotics: Science and Systems*. Freiburg im Breisgau, Germany. doi:10.15607/RSS.2019.XV.054.
- Proctor, J.L., Brunton, S.L., and Kutz, J.N. (2018). Generalizing Koopman Theory to Allow for Inputs and Control. *SIAM Journal on Applied Dynamical Systems*, 17(1), 909–930. doi:10.1137/16M1062296.
- Rubagotti, M., Incremona, G.P., Raimondo, D.M., and Ferrara, A. (2021). Constrained Nonlinear Discrete-Time Sliding Mode Control Based on a Receding Horizon Approach. *IEEE Transactions on Automatic Control*, 66(8), 3802–3809. doi:10.1109/TAC.2020.3024349.
- Sotiropoulos, F.E. and Asada, H.H. (2022). Dynamic Modeling of Bucket-Soil Interactions Using Koopman-DFL Lifting Linearization for Model Predictive Contouring Control of Autonomous Excavators. *IEEE Robotics and Automation Letters*, 7(1), 151–158. doi:10.1109/LRA.2021.3121136.
- Surana, A. (2016). Koopman operator based observer synthesis for control-affine nonlinear systems. In *2016 IEEE 55th Conference on Decision and Control (CDC)*, 6492–6499. doi:10.1109/CDC.2016.7799268.
- Williams, M.O., Hemati, M.S., Dawson, S.T., Kevrekidis, I.G., and Rowley, C.W. (2016). Extending Data-Driven Koopman Analysis to Actuated Systems. *IFAC-PapersOnLine*, 49(18), 704–709. doi:10.1016/j.ifacol.2016.10.248. 10th IFAC Symposium on Nonlinear Control Systems NOLCOS 2016.
- Zheng, Y., Dimirovski, G.M., Jing, Y., and Yang, M. (2007). Discrete-Time Sliding Mode Control of Nonlinear Systems. In *2007 American Control Conference*, 3825–3830. doi:10.1109/ACC.2007.4282412.
- Zinage, V. and Bakolas, E. (2022). Koopman Operator Based Modeling and Control of Rigid Body Motion Represented by Dual Quaternions. In *2022 American Control Conference (ACC)*, 3997–4002. doi:10.23919/ACC53348.2022.9867584.

Appendix A. TRANSFORMATION TO REGULAR FORM

The procedure presented in Edwards and Spurgeon (1998) is used. Given $x^+ = \mathbf{A}x + \mathbf{B}u$, $y = \mathbf{C}x$, $x \in \mathbb{R}^n$, $y \in \mathbb{R}^p$, $u \in \mathbb{R}$, define $z = \mathbf{T}_1x$, where

$$\mathbf{T}_1 = [\mathbf{W}^T \mathbf{C}], \quad (\text{A.1})$$

and the columns of \mathbf{W} span the null-space of \mathbf{C} . Applying this transformation leads to $\mathbf{T}_1\mathbf{B} = [\mathbf{B}_{c1} \mathbf{B}_{c2}]^T$ where $\mathbf{B}_{c1} \in \mathbb{R}^{(n-p) \times 1}$, $\mathbf{B}_{c2} \in \mathbb{R}^{p \times 1}$. Perform the QR decomposition to yield $\mathbf{B}_{c2} = \mathbf{Q}\mathbf{R}$, where $\mathbf{Q} \in \mathbb{R}^{p \times p}$ is an orthogonal matrix and \mathbf{R} is upper-triangular. Rearrange \mathbf{Q} and \mathbf{R} , to yield \mathbf{Q}_s and \mathbf{R}_s , so that \mathbf{R}_s is now lower triangular.

Define the second transformation $v = \mathbf{T}_2z$, where

$$\mathbf{T}_2 = \begin{bmatrix} \mathbf{I}_{(n-p)} & -\mathbf{B}_{c1}\mathbf{B}_{c2}^\dagger \\ 0 & \mathbf{Q}_s^T \end{bmatrix}, \quad (\text{A.2})$$

and $\mathbf{B}_{c2}^\dagger = (\mathbf{B}_{c2}^T\mathbf{B}_{c2})^{-1}\mathbf{B}_{c2}^T$ is the pseudo-inverse of \mathbf{B}_{c2} . Thus, the dynamics in the regular form is given by

$$v^+ = \mathbf{T}_2\mathbf{T}_1\mathbf{A}\mathbf{T}_1^{-1}\mathbf{T}_2^{-1}v + \mathbf{T}_2\mathbf{T}_1\mathbf{B}u, \quad (\text{A.3})$$

where

$$\mathbf{T}_2\mathbf{T}_1\mathbf{A}\mathbf{T}_1^{-1}\mathbf{T}_2^{-1} = \begin{bmatrix} \mathbf{A}_{11} & \mathbf{A}_{12} \\ \mathbf{A}_{21} & \mathbf{A}_{22} \end{bmatrix} \quad (\text{A.4})$$

and

$$\mathbf{T}_2\mathbf{T}_1\mathbf{B} = \begin{bmatrix} 0 \\ \mathbf{B}_2 \end{bmatrix} \quad (\text{A.5})$$